# All-polymeric flexible transparent heaters

Magatte Gueye, Alexandre Carella, Renaud Demadrille, Jean-Pierre Simonato

# All-polymeric flexible transparent heaters

*Magatte N. Gueye[†‡], Alexandre Carella[†]*, Renaud Demadrille[‡] and Jean-Pierre Simonato[†]*.*

[†]Univ. Grenoble Alpes, CEA, Liten, DTNM, SEN, LSIN, F-38000 Grenoble, France.

[‡]Univ. Grenoble Alpes, CEA, CNRS, INAC, SYMMES, CNRS, F-38000 Grenoble, France.

KEYWORDS. organic transparent heaters, PEDOT, transparent conductive materials, thin film heaters, conducting polymers.

ABSTRACT. All-polymeric flexible transparent heaters are demonstrated for the first time. Thin films of four poly(3,4-ethylenedioxythiophene) (PEDOT) based materials embedding different dopants exhibit low sheet resistances, down to 57 Ω $sq^{-1}$ associated with good transparencies (> 87 %) and a haze lower than 1 %. These transparent thin films show excellent heating properties, with high heating rates (up to 1.6 °C $s^{-1}$) and steady state temperatures exceeding 100 °C when subjected to a 12 V bias. Very high areal power densities were also measured, reaching almost 10 000 W $m^{-2}$. The temperature rises are finely fitted with a thermal model. It is further demonstrated that these new transparent heaters can be efficiently integrated for applications in thermochromic displays and visor deicers.

## 1. Introduction

Transparent heaters (THs) are one of the main applications of transparent conductive materials (TCMs) in which heat is produced by Joule effect when a voltage is applied. The first use of these materials dates back from the World War II when they were applied for defrosting the windows of airplanes at high altitudes.[1] Nowadays indium tin oxide (ITO) is the most employed TCM in general and for TH in particular, the foremost uses being for defrosters and defoggers in vehicles, advertisement boards, avionics and displays.[1–3] Due to the growing market of TCMs and the increasing demand on flexible devices, the brittleness of ITO and the scarcity of indium stimulated research for alternative materials. In that respect, THs made of metal oxides, carbon nanotubes, graphene, metallic nanowires (NWs), metal meshes and hybrid materials have been investigated.[4–15] After seminal studies focused only on metal oxides, carbon nanotubes (CNTs) and graphene based heaters refreshed the attention on THs.[16–18] The high sheet resistances in CNTs require however a too high input voltage and the numerous defects in graphene induce some local hot spots and hence a non-uniform heating over large areas. Unfortunately, these materials do not allow to reach excellent trade-off between conductivity and transparency and require high bias to be activated. Metallic nanowire-based networks were proved to be efficient THs only few years ago.[7,19] They are solution-processable and exhibit low sheet resistance, high transparency, excellent flexibility and hence are convenient for flexible transparent film heaters.[2,3,7,20–22] Hybridizing AgNWs with conducting polymers such as poly(ethylenedioxythiophene: polystyrenesulfonate) (PEDOT:PSS) allows to reduce the sheet resistance and to homogenize the heating.[10] However, it was demonstrated that these hybrids show moderate stability.[23–25] Conducting polymers are well-known to be relevant TCMs for OLEDs, photovoltaics, sensors and other optoelectronics devices.[11,26–28] Some PEDOT

derivatives are commercially available, and recent reports in this field have shown that thin films of PEDOT can reach very high conductivities, of up to 5400 S $cm^{-1}$.[28–43]

Surprisingly, to the best of our knowledge, no TH solely based on conducting polymers has ever been reported, although these materials can exhibit outstanding optoelectrical properties and interesting thermal response.[31,44,45] Here we demonstrate that all-polymeric transparent thin films can be used as TH, with excellent heating properties and very good optoelectronic figure of merit. The obtained results rank them at the very best level when compared to the state of the art materials.

## 2. Results and discussion

This study was carried out with four different polymers based on PEDOT. Commercial PEDOT:PSS (Clevios PH1000) was used as deposited, or after being treated with ethylene glycol, which is known to increase carrier density and the carrier mobility (this material was named PEDOT:PSS-EG).[46,47] Two other PEDOT materials, namely PEDOT:OTf and PEDOT:Sulf, with conductivities exceeding respectively 3000 S $cm^{-1}$ and 5000 S $cm^{-1}$ were also used for this study.[39] To the best of our knowledge, PEDOT:Sulf owns the highest conductivity reported so far for PEDOT-based thin films. Chemical structures of these polymers are represented in Figure 1a,b,c. Besides their outstanding electrical properties, these materials also exhibit high transparencies in the visible spectrum, which are two key properties for transparent thin film heaters. Their main optoelectrical properties are reported in Figure 1d,e. The high conductivity associated to the low thickness of PEDOT:OTf and PEDOT:Sulf films are at the origin of the excellent trade-off between sheet resistance and high transparency in the visible range. PEDOT:PSS and PEDOT:PSS-EG on the other hand are less conductive materials (178

and 1361 S $cm^{-1}$ respectively), which is mainly due to the excess of insulating PSS present in the films. However, this excess of PSS does not absorb in the visible range, and hence is not detrimental for the transparency of these materials. Figure 1d shows the specular transmission values at 550 nm of the four materials as a function of their sheet resistances. Transparencies higher than 80 % associated with sheet resistances below 100 Ω $sq^{-1}$ are very good features to achieve high performance THs.[3] This can be easily accomplished by stacking two to three layers of PEDOT films. In addition to these optoelectrical properties, these materials barely diffuse light, as evidenced by the very low haze factor which remains below 1 % in the entire visible range (Figure 1e). All the proper prerequisites being met, it was therefore appealing to evaluate the heating performances of transparent thin films of PEDOT:PSS, PEDOT:PSS-EG, PEDOT:OTf and PEDOT:Sulf.

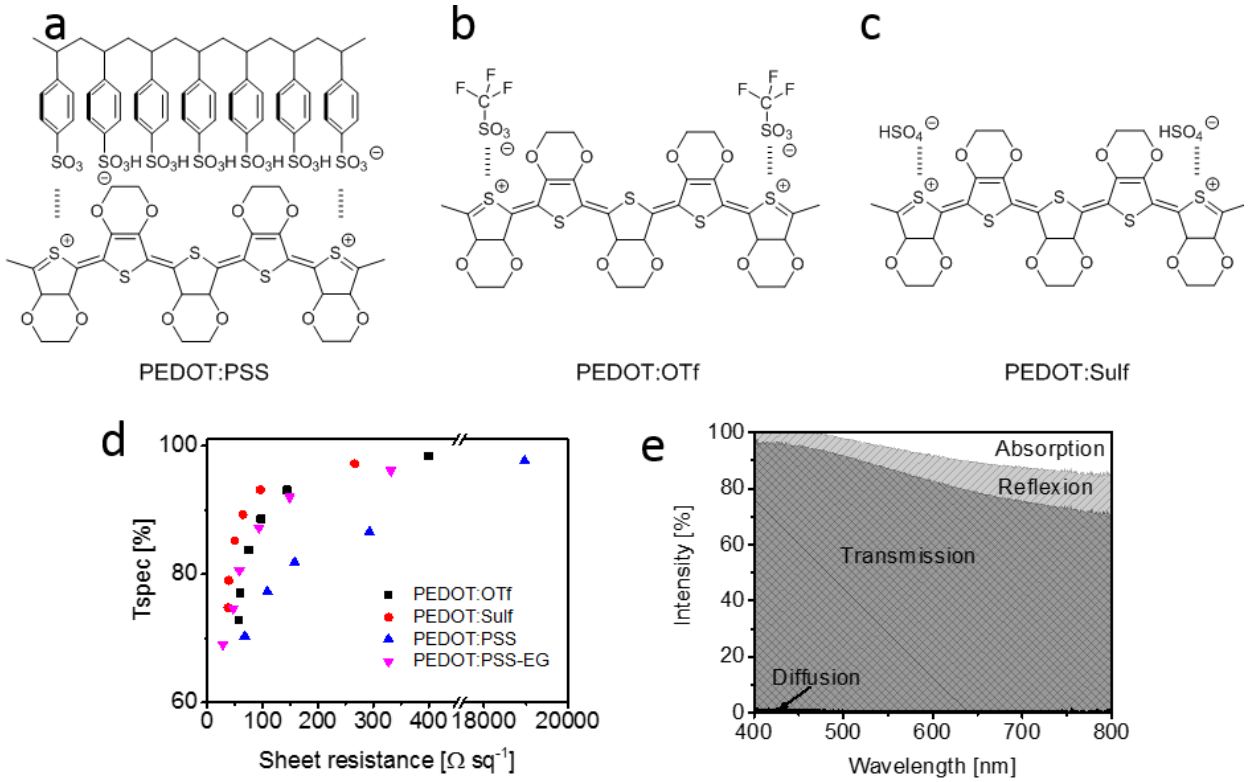

**Figure 1.** PEDOT materials and their optoelectrical properties. a) PEDOT:PSS. b) PEDOT:OTf. c) PEDOT:Sulf. d) Dependence of the transmittance at 550 nm as function of the sheet resistance of the materials. e) Optical properties of PEDOT:Sulf in the visible range. ($Haze = (Diffuse\ transmittance)/(Total\ transmittance)$ <1 %).

### 2.1. Experimental observation of the heating performances

THs were fabricated by spin-coating PEDOT-based materials on 25x25 mm² glass substrates and small strips of silver ink were deposited on the opposing edges of the materials in order to ensure a better contact between the films and the external circuit (see Figure S1 in the Supporting Information SI).

**Table 1.** Optical, electrical and heating properties of the studied PEDOT based materials.

| Materials | Sheet resistance [$\Omega$ sq$^{-1}$] | Total transmission @ 550 nm [%] | Haze [%] | FOM[a] | Temperature at 10 V [°C] | Heating rate at 10 V [°C s$^{-1}$] |
|---|---|---|---|---|---|---|
| PEDOT:PSS | 361 | 90.1 | 0.1 | 10 | 45 | 0.2 |
| PEDOT:PSS-EG | 68 | 89.6 | 0.7 | 49 | 94 | 1.0 |
| PEDOT:OTf | 81 | 88.4 | 0.5 | 37 | 88 | 0.9 |
| PEDOT:Sulf | 57 | 87.8 | 0.7 | 50 | 114 | 1.2 |

[a] FOM as from Coleman *et al.*[48] $FOM = \frac{\sigma_{DC}}{\sigma_{OP}} = \frac{Z_0}{2R_S(T^{-1/2}-c)}$ with $Z_0$ = impedance of free space = 377 Ω, T the transmittance, Rs the sheet resistance, $\sigma_{DC}$ the electrical conductivity and $\sigma_{OP}$ the optical conductivity.

In order to assess the performances of these PEDOT-based materials as THs, voltages from 4 to 12 V were applied on the four films. The main optical, electrical and heating properties are summarized in Table 1. The temperature elevation, as recorded with a K-type thermocouple affixed under the substrate for all four materials, is displayed in Figure 2a,b,d,e. The IR image of a TH in Figure 2c gives an illustration of the temperature rise throughout the film and the connecting wires. PEDOT:PSS, whose resistance is the highest, shows the poorest temperature increase (Figure 2b). At 10 V bias, PEDOT:OTf and PEDOT:PSS-EG have performances twice higher than PEDOT:PSS (Figure 2a,e), reaching 88 °C and 94 °C respectively. PEDOT:Sulf shows even better heating properties reaching 120 °C at 10 V bias, and 138 °C at 12 V bias. Though the possibility to heat at temperatures above 200°C was demonstrated (Figure S3), we focused the study in a temperature range below 100°C, which is more consistent with the targeted applications, *i.e.* defogging and thermochromic displays.

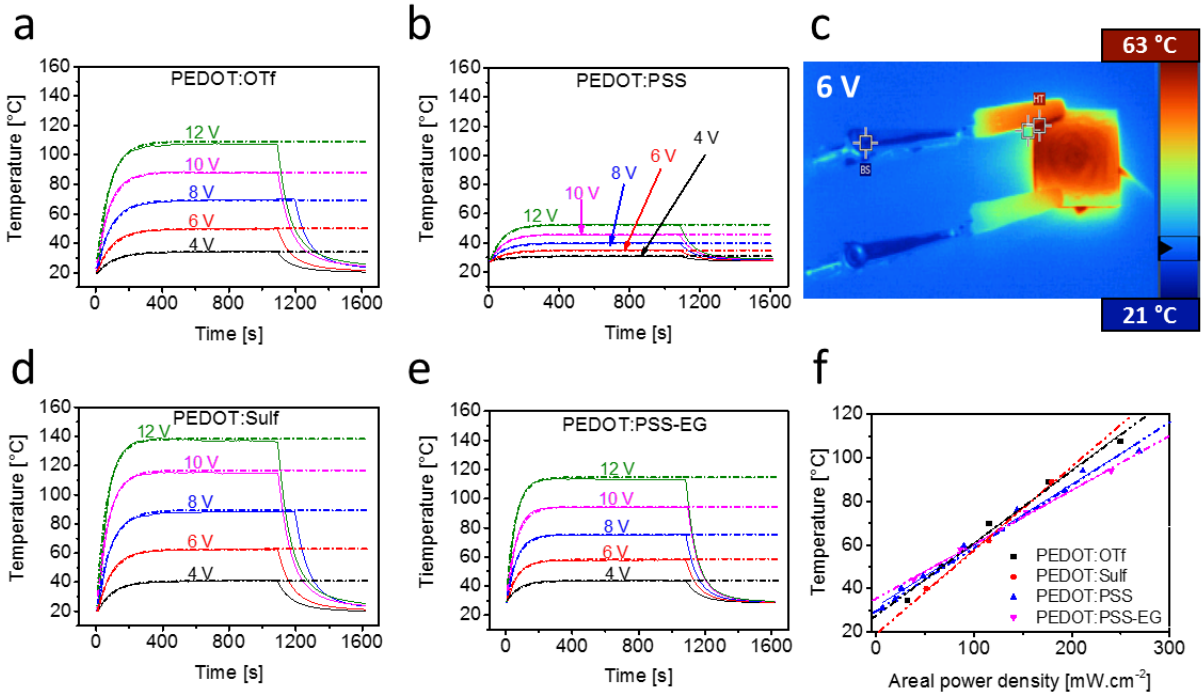

**Figure 2.** Heating performances of PEDOT based THs. a,b,d,e) Temperature elevation of PEDOT-based materials deposited by spin-coating on glass substrates. Voltages from 4 to 12 V were applied and shut off after ca. 1000 – 1200 s. Curves were fitted with the model from Equation 1. Solid lines represent the experimental curves and dash lines the calculated fits. c) IR image of a PEDOT:PSS-EG based TH heated at 63 °C (applied voltage = 6 V). The heat losses in the electrodes' contacts (left side), the thermocouple's wire (right side) and the Kapton® tape (lower side) are visible. d) Areal power density of PEDOT-based THs.

The trend of the heating ability can be correlated with the electrical resistances, but could also be correlated with the figure of merit (FOM) as introduced by Coleman and coworkers (see Table 1).[48] The FOM is basically a relationship between the transmittance T and the sheet resistance Rs that is controlled by the conductivity ratio, $\sigma_{DC}/\sigma_{OP}$. The FOM is therefore a good indicator to rank different materials.[48,49] It appears in Table 1 that PEDOT:PSS-EG and PEDOT:Sulf have equivalent optoelectrical properties. In other words if equivalent transmittances are achieved, the same thermal responses would likely be achieved as well. The better thermal responses are however obtained with PEDOT:Sulf whose resistance is the lowest. The FOM still remains the most adequate tool to classify them and despite their different conductivities, PEDOT:Sulf and PEDOT:PSS-EG seem to have equivalent TH's properties.

Based on those results, it appears that PEDOT-based materials are very competitive in the field of THs with heating properties even better than those of CNTs, graphene and metal oxides and comparable to that of silver nanowires and derived hybrids.[3,17,18] Beside the temperature elevation, the response time as well as the stability of the TH are parameters to be dealt with

before considering potential industrial applications. To this goal, experimental data were recorded and compared to a theoretical model.

### 2.2. Modelling the temperature elevation

Being able to theoretically anticipate the temperature elevation in these PEDOT films would allow a fine tuning of the properties' choice at an applied voltage in order to optimize the TH system. Sorel et al. developed a relevant and comprehensive model that describes the temperature dependence of the system {material + substrate} with their characteristics.[49] That model was given for silver nanowires networks but can be extended to our polymer films as it is an energy balance between the dissipated power by Joule heating and the power losses through conduction, convection and radiation. When applying a voltage $U$ to a film, a current $I$ flows through it and the power dissipated by Joule heating is given by $P_{Joule} = RI^2 = \frac{U^2}{R}$, assuming that the sample does not alter with time (which is the case, see the stable thermal responses in Figure 2). That heat is dissipated *via* conduction, hence raising the temperature of both the material and its substrate, *via* convection and *via* radiation. By neglecting the losses through the electrodes, thermocouples and other wires in the circuits and assuming a uniform temperature all over the sample, the energy balance is given by Equation 1.

$$\frac{\boldsymbol{U^2}}{\boldsymbol{R}} = (\boldsymbol{m_1 C_1 + m_2 C_2})\frac{\boldsymbol{dT(t)}}{\boldsymbol{dt}} + \boldsymbol{A(h_1 + h_2)(T(t) - T_0)} + \boldsymbol{\sigma A}(\varepsilon_1 + \varepsilon_2).(\boldsymbol{T(t)^4 - T_0{}^4}) \qquad \textbf{(1)}$$

The indexes 1 and 2 refer to the PEDOT material and the substrate respectively. $C_1$ and $C_2$ are the specific heat capacities, $m_1$ and $m_2$ the masses, $h_1$ and $h_2$ the convective heat transfer coefficients and $\varepsilon_1$ and $\varepsilon_2$ the emissivities from both sides of the studied system. $\sigma$ is the Stefan-

Boltzmann constant and A the area of the film. T(t) is the instantaneous temperature and $T_0$ the ambient temperature. Since $m_1 \ll m_2$, the conduction loss term can be reduced, hence giving $mC\frac{dT(t)}{dt}$. Moreover, as such equation does not have any simple analytical solution, it is simplified by hypothesizing small temperature variations and by applying a Taylor expansion that gives $T(t)^4 - {T_0}^4 \approx 4T_0^3(T(t) - T_0)$. The following solution can be demonstrated:

$$\boldsymbol{T(t) = T_0 + \frac{1}{\alpha}.\frac{U^2}{RA}.\left(1 - e^{-\frac{\alpha A}{mc}t}\right)} \qquad \textbf{(2)}$$

Here, $\alpha = (h_1 + h_2) + 4T_0^3(\varepsilon_1 + \varepsilon_2)$ and stands for the heat transfer coefficient related to convection and conduction losses.

Equation 2 was used to fit the temperature elevation curves in Figure 2a,b,c,d. The dashed lines corresponding to the calculated fits are superposed to experimental data. Thus it appears that the model reflects quite accurately the heating capability of the PEDOT-based materials and the rare deviations observed, particularly above 80 °C, can be attributed to the hypotheses of the model. At steady state temperature, the temperature depends solely on the areal power density $\frac{U^2}{RA}$ and the heat transfer constant $\alpha$. That linear dependency is shown in Figure 2f and $\alpha$ was found to be 28, 25, 33 and 38 W $m^{-2}$ $K^{-1}$ respectively for PEDOT:PSS, PEDOT:PSS-EG, PEDOT:OTf and PEDOT:Sulf. These values are comparable to those reported for silver nanowire based film heaters.[20,49]

In the linear dependency region, areal power densities up to 240 mW $cm^{-2}$ were reached for PEDOT:PSS-EG under 10 V bias. This power density can be further increased up to near 1000 mW $cm^{-2}$, i.e. 10 000 W $m^{-2}$, when 22 V are applied, the steady state temperature being then 214

°C (Figure S3). Even though high steady state temperature (> 200 °C) and very high areal power density can be achieved, these conditions are not recommended because of potential degradation of the organic polymer.

As the steady state temperature depends on the areal power density, moving to large areas THs will inevitably induce a drop of heating performances unless the total resistance of the TH is modulated, geometrically for instance. Indeed, the temperature responses of two PEDOT:Sulf based TH deposited on a 25x25 mm² and a 100x100 mm² glass substrate were compared (Figure S2). For a 16 times larger surface, a 4 times higher voltage is required, all other properties being unchanged.

Thanks to these experiments, PEDOT-based films proved to be suitable for TH applications at low voltages, and are even scalable as long as the TH device is designed in a way to minimize the total electrical resistance. The properties making a good TH are not restricted to low electrical resistivity at a high transparency (and low haze factor). The THs should in addition have a fair response time for practical applications, high thermal stability and a good resistance to environmental stresses.

### 2.3. Heating rate

Heating rates for THs based on graphene, CNTs or metallic nanowires are typically in the range 0.1 to 2.0 °C $s^{-1}$ for low voltage bias (< 12 V).[3,7,16] Table 1 gives the steady state temperatures and the maximum heating rates when 10 V are applied on our all-polymeric THs. At such bias the heating rate ranges from 0.2 °C $s^{-1}$ for PEDOT:PSS to 1.2 °C $s^{-1}$ for PEDOT:Sulf. This parameter is material dependent and temperature dependent (Figure S5) and it can be as high as 4 °C $s^{-1}$ for PEDOT:PSS-EG when 22 V are applied. At such heating rates, the steady state

temperature is reached after less than *ca.* 400 s for all materials, which can be observed in Figure 2a,b,c,d. The response time of THs can be measured using the 99 % response time ($t_{99\,\%}$) which is the time needed to reach 99 % of the steady state temperature. It is given by $t_{99\,\%} = 2\frac{mC}{\alpha A}\ln 10$, deduced from Equation 2, which is theoretically between 270 and 400 s for all for materials, given the heat transfer constants found previously and the mass and specific capacity of the glass substrate. This is consistent with observations in Figure 2. This concordance between the experiments and the theory confirms the relevance of the model and sheds some light on the parameters that could improve the response time of these PEDOT based THs. In other words, given the thin thickness of PEDOT films, the time response is mainly function of the substrate's properties (mass, area and specific heat capacity). Thus, heavier, larger or less thermally conductive substrates will induce a longer response time. Therefore, compared to the 1 mm thick glass substrate, a 125 µm PET (Polyethylene terephthalate) substrate will show faster thermal response times (Figure S4). It is interesting to note that depositing PEDOT on thin PET substrate (125 µm) not only increases the response time as expected, but also leads to a flexible TH.

### 2.4. Stability

Heating and cooling cycles on PEDOT based THs have been performed. Representative experimental results are shown in Figure 3a for PEDOT:PSS-EG; the data for the three other polymers are presented in Figure S6. The active materials were deposited on 25x25 mm² glass substrates and the required voltages to reach a 50 °C steady state temperature were applied and shut down every 400 s. No significant changes were noticed and the temperature remained stable after 20 cycles for each PEDOT based material. PEDOT:PSS-EG and PEDOT:Sulf, which are the materials possessing the best THs' properties, were also subjected to a constant bias for 200 h

(i.e. continuously for more than 8 days), targeting a 50 °C steady state temperature. The results are given in Figure 3b and in Figure S7. It was observed that under constant bias stress, PEDOT:PSS-EG heating capability decreases from 63 °C to 54 °C (-15 %). The reasons for this moderate drop have not been clearly established so far, but PEDOT materials are known to be moisture-sensitive.[50] Consequently we decided to encapsulate the TH with a film barrier, whose WVTR (water vapor transmission rate) is given at $5.10^{-5}$ g $m^{-2}$ $d^{-1}$ at 40 °C and 90 % RH, and which adhered to the film through an optically clear adhesive.[51] It resulted in an obvious stabilization of the functional system, less than 1 °C variation being observed after 200h.

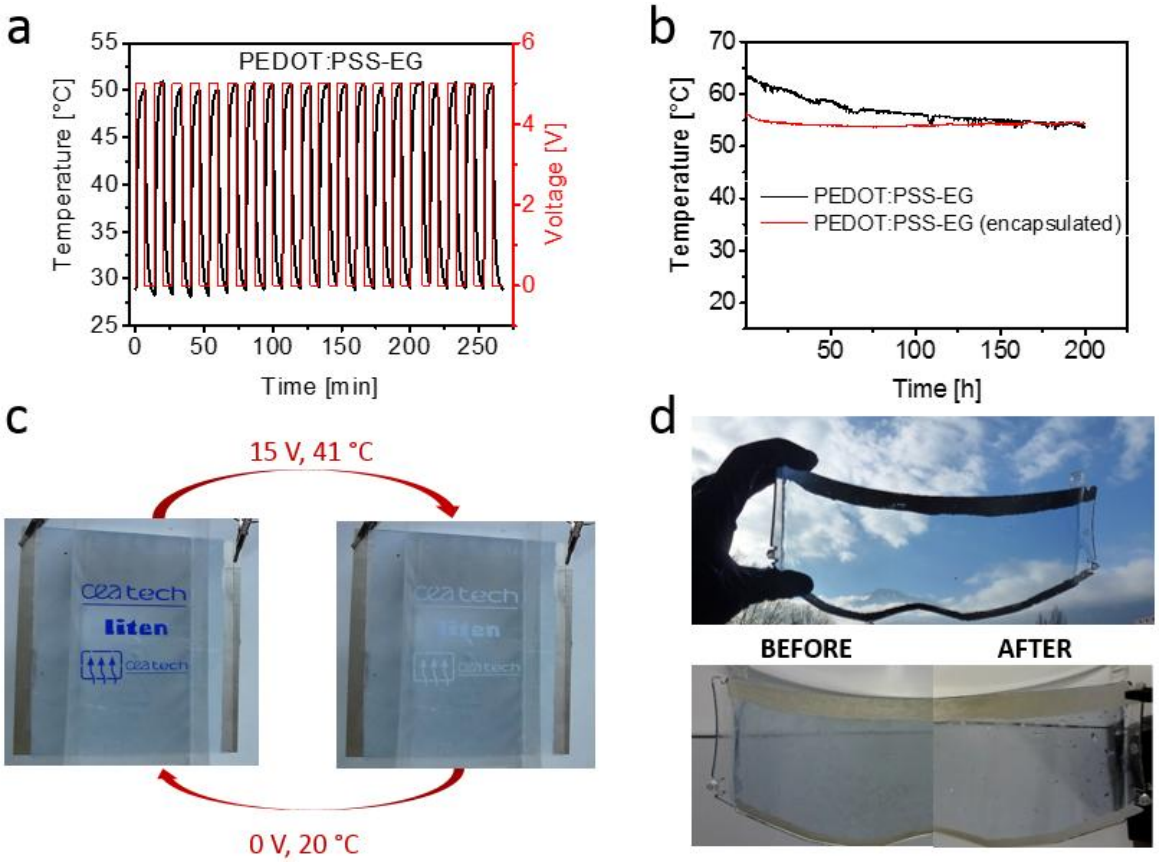


**Figure 3.** a) Stability of PEDOT:PSS-EG through cycling. All four materials show similar behavior, details are in the SI. b) Stability of PEDOT:PSS-EG with and without encapsulation

when a constant voltage is applied for 8 days (U = 6 V). c) Application as thermochromic display. d) Application as visor deicer.

### 2.5. Applications

Development of polymeric THs is particularly beneficial because PEDOT polymers are easily processable. Consequently large area, flexible and curved devices can be built easily and at significantly lower cost when compared to TCOs. As a matter of fact, PEDOT dispersion or oxidative solution can be deposited on flexible substrates, for instance transparent polymer films such as PET. Their thermal properties are even better as explained hereinbefore, and demonstrated in Figure S4. For practical applications we performed more than 1000 flexions at 10 mm bending radius, on a 100x100 mm² PEDOT:PSS-EG based TH (Figure S8) without altering the THs heating properties.

In order to demonstrate the interest of PEDOT in future TH applications, integration in thermochromic displays (on glass) and visor defoggers/deicers (on polymer substrate) has been carried out. Figure 3c shows a thermochromic display. PEDOT:Sulf was deposited on a 100x100 mm² glass substrate (58 Ω $sq^{-1}$, 88 % transmittance). The thermochromic ink (activation temperature 43°C) was spray-coated through a shadow mask on a film barrier. The latter was used to encapsulate the PEDOT thin film. When 15 V bias is applied, the temperature increases until the pattern color turns from blue to white at 43 °C. When the voltage is switched off, the temperature decreases, inducing the recovery of the blue color. This was realized for dozens of cycles without any alteration. In the second example of application PEDOT:PSS-EG was drop-coated on a motorcycle visor (20 Ω $sq^{-1}$, 92 % transmittance, Figure 3d). The external surface

was then slightly humidified and the visor was iced in a fridge at -10 °C. Deicing was then performed in few seconds by applying 15 V to heat up the surface. These demonstrators evidence the relevant use of PEDOT based thin films as THs. It is noteworthy that this technology combines excellent TH properties and easy deposition process on large, curved or flexible substrates.

## 3. Conclusions

In summary, transparent heaters based on thin films of PEDOT polymers are demonstrated for the first time. In particular, PEDOT:Sulf depicts outstanding properties, with a sheet resistance of 57 $\Omega$ $sq^{-1}$ at 87.8 % transmittance, 1.6 °C $s^{-1}$ heating rate and a steady state temperature of 138 °C under 12 V bias.

It is also shown that THs can be realized from commercially available PEDOT:PSS solutions. For instance PEDOT:PSS-EG (68 $\Omega$ $sq^{-1}$ at 89.6 % transmittance), shows also excellent heating performances, and stability after cycling and after 200 h at 50 °C was evidenced. Very high areal power density was measured with this material, reaching up to 10 000 W $m^{-2}$. Thanks to a straightforward deposition process, in particular on large and curved surfaces such as visor, the PEDOT transparent thin films can be integrated into various functional devices, such as thermochromic displays or de-icing of visors. After metal oxides, CNTs, graphene, metallic nanowires, metal meshes and hybrids, conducting polymers stand as the next generation of low cost, easily processable, flexible transparent heaters.

ASSOCIATED CONTENT

**Supporting Information**. Experiment details can be found in the Supporting information, as well as additional figures. Figure S1: Different pictures of the samples. Table S1: electrical properties of the materials. Figure S2 to Figure S5: heating properties as function of the substrate characteristics. Figure S6 and Figure S7: Stability and ageing. Figure S8: Flexible TH. This material is available free of charge via the internet at http://pubs.acs.org/ (file type PDF).

AUTHOR INFORMATION

**Corresponding Author**

*Authors to whom correspondence should be addressed: alexandre.carella@cea.fr, jean-pierre.simonato@cea.fr.

**Present Addresses**

[†]Univ. Grenoble Alpes, CEA, Liten, DTNM, SEN, LSIN, F-38000 Grenoble, France.

[‡]Univ. Grenoble Alpes, CEA, CNRS, INAC, SYMMES, CNRS, F-38000 Grenoble, France.

**Author Contributions**

The manuscript was written through contributions of all authors. All authors have given approval to the final version of the manuscript.

**Funding Sources**

The authors acknowledge the LABEX Laboratoire d'Alliances Nanosciences-Energies du Futur (LANEF, ANR-10-LABX-51- 01) for funding the MNG Ph.D.

REFERENCES


(1) Gordon, R. G. Criteria for Choosing Transparent Conductors. *MRS Bull.* **2000**, *25* (8), 52–57.

(2) Sannicolo, T.; Lagrange, M.; Cabos, A.; Celle, C.; Simonato, J.; Bellet, D. Metallic Nanowire-Based Transparent Electrodes for Next Generation Flexible Devices : A Review. *Small* **2016**, *12* (144), 6052–6075.

(3) Gupta, R.; Rao, K. D. M.; Kiruthika, S.; Kulkarni, G. U. Visibly Transparent Heaters. *ACS Appl. Mater. Interfaces* **2016**, *8* (20), 12559–12575.

(4) Kim, J. H.; Ahn, B. Du; Kim, C. H.; Jeon, K. A.; Kang, H. S.; Lee, S. Y. Heat Generation Properties of Ga Doped ZnO Thin Films Prepared by Rf-Magnetron Sputtering for Transparent Heaters. *Thin Solid Films* **2008**, *516* (7), 1330–1333.

(5) Jang, H.; Jeon, S. K.; Nahm, S. H. The Manufacture of a Transparent Film Heater by Spinning Multi-Walled Carbon Nanotubes. *Carbon* **2011**, *49* (1), 111–116.

(6) Bae, J. J.; Lim, S. C.; Han, G. H.; Jo, Y. W.; Doung, D. L.; Kim, E. S.; Chae, S. J.; Huy, T. Q.; Luan, N. Van; Lee, Y. H. Heat Dissipation of Transparent Graphene Defoggers. *Adv. Funct. Mater.* **2012**, *22* (21), 4819–4826.

(7) Celle, C.; Mayousse, C.; Moreau, E.; Basti, H.; Carella, A.; Simonato, J. P. Highly Flexible Transparent Film Heaters Based on Random Networks of Silver Nanowires. *Nano Res.* **2012**, *5* (6), 427–433.

(8) Zhai, H.; Wang, R.; Wang, X.; Cheng, Y.; Shi, L.; Sun, J. Transparent Heaters Based on Highly Stable Cu Nanowire. *Nano Res.* **2016**, *9* (12), 3924–3936.

(9) Chen, J.; Chen, J.; Li, Y.; Zhou, W.; Feng, X.; Huang, Q.; Zheng, J.; Liu, R.; Ma, Y.; Huang, W. Enhanced Oxidation-Resistant Cu–Ni Core–shell Nanowires: Controllable One-Pot Synthesis and Solution Processing to Transparent Flexible Heaters. *Nanoscale* **2015**, *7* (40), 16874–16879.

(10) Ji, S.; He, W.; Wang, K.; Ran, Y.; Ye, C. Thermal Response of Transparent Silver Nanowire / PEDOT : PSS Film Heaters. *Small* **2014**, *10* (23), 4951–4960.

(11) Hecht, D. S.; Hu, L.; Irvin, G. Emerging Transparent Electrodes Based on Thin Films of Carbon Nanotubes , Graphene , and Metallic Nanostructures. *Adv. Mater.* **2011**, *23* (13), 1482–1513.

(12) Gupta, R.; Walia, S.; Jensen, J.; Angmo, D.; Krebs, F. C.; Kulkarni, G. U. Solution Processed Large Area Fabrication of Ag Patterns as Electrodes for Flexible Heaters, Electrochromics and Organic Solar Cells. *J. Mater. Chem. A* **2014**, *2* (28), 10930–10937.

(13) Gao, T.; Wang, B.; Ding, B.; Lee, J.; Leu, P. W. Uniform and Ordered Copper Nanomeshes by Microsphere Lithography for Transparent Electrodes. *Nano Lett.* **2014**, *14* (4), 2105–2110.

(14) Lan, W.; Chen, Y.; Yang, Z.; Han, W.; Zhou, J.; Zhang, Y.; Wang, J.; Tang, G.; Wei, Y.; Dou, W.; Su, Q.; Xie, E. Ultra Flexible Transparent Film Heater Made of Ag Nanowire/PVA Composite for Rapid-Response Thermotherapy Pads. *ACS Appl. Mater. Interfaces* **2017**, *9* (7), 6644–6651.

(15) Lordan, D.; Burke, M.; Manning, M.; Martin, A.; Amann, A.; Connell, D. O.; Murphy, R.; Lyons, C.; Quinn, A. J. Asymmetric Pentagonal Metal Meshes for Flexible Transparent Electrodes and Heaters. *ACS Appl. Mater. Interfaces* **2017**, *9* (5), 4932–4940.

(16) Janas, D.; Koziol, K. K. A Review of Production Methods of Carbon Nanotube and Graphene Thin Films for Electrothermal Applications. *Nanoscale* **2014**, *6* (6), 3037–3045.

(17) Kang, J.; Kim, H.; Kim, K. S.; Lee, S.-K.; Bae, S.; Ahn, J.-H.; Kim, Y.; Choi, J.; Hong, B. H. High-Performance Graphene-Based Transparent Flexible Heaters. *Nano Lett.* **2011**, *11* (12), 5154–5158.

(18) Sui, D.; Huang, Y.; Huang, L.; Liang, J.; Ma, Y.; Chen, Y. Flexible and Transparent Electrothermal Film Heaters Based on Graphene Materials. *Small* **2011**, *7* (22), 3186–3192.

(19) Simonato, J. P.; Celle, C.; Mayousse, C.; Carella, A.; Basti, H.; Carpentier, A. Transparent Film Heaters Based on Silver Nanowire Random Networks. *MRS Proc.* **2012**, *1449* (12), 107–113.

(20) Lagrange, M.; Sannicolo, T.; Lohan, B. G.; Khan, A.; Anikin, M.; Jiménez, C.; Bruckert, F.; Bréchet, Y.; Bellet, D. Understanding the Mechanisms Leading to Failure in Metallic Nanowire-Based Transparent Heaters , and Solution for Stability Enhancement. *Nanotechnology* **2017**, *28* (5), 055709.

(21) Lee, S. M.; Lee, J. H.; Bak, S.; Lee, K.; Li, Y.; Lee, H. Hybrid Windshield-Glass Heater for Commercial Vehicles Fabricated via Enhanced Electrostatic Interactions among a Substrate , Silver Nanowires , and an over-Coating Layer. *Nano Res.* **2015**, *8* (6), 1882–1892.

(22) Kim, T.; Kim, Y. W.; Lee, H. S.; Kim, H.; Yang, W. S.; Suh, K. S. Uniformly Interconnected Silver-Nanowire Networks for Transparent Film Heaters. *Adv. Funct. Mater.* **2013**, *23* (10), 1250–1255.

(23) Mayousse, C.; Celle, C.; Fraczkiewicz, A.; Simonato, J. Stability of Silver Nanowire Based Electrodes under Environmental and Electrical Stresses. *Nanoscale* **2015**, *7* (5), 2107–2115.

(24) Chen, S.; Song, L.; Tao, Z.; Shao, X.; Huang, Y.; Cui, Q.; Guo, X. Neutral-pH PEDOT : PSS as over-Coating Layer for Stable Silver Nanowire Flexible Transparent Conductive Films. *Org. Electron.* **2014**, *15* (12), 3654–3659.

(25) Choi, D. Y.; Kang, H. W.; Sung, H. J.; Kim, S. S. Annealing-Free, Flexible Silver Nanowire – Polymer Composite Electrodes via a Continuous Two-Step Spray-Coating Method. *Nanoscale* **2013**, *5* (3), 977–983.

(26) Argun, B. A. A.; Cirpan, A.; Reynolds, J. R. The First Truly All-Polymer Electrochromic Devices. *Adv. Mater.* **2003**, *15* (15), 1338–1341.

(27) Kirchmeyer, S.; Reuter, K. Scientific Importance , Properties and Growing Applications of poly(3,4-Ethylenedioxythiophene). *J. Mater. Chem.* **2005**, *15* (21), 2077–2088.

(28) Hojati-Talemi, P.; Bächler, C.; Fabretto, M.; Murphy, P.; Evans, D. Ultrathin Polymer Films for Transparent Electrode Applications Prepared by Controlled Nucleation. *ACS Appl. Mater. Interfaces* **2013**, *5* (1), 11654–11660.

(29) Xia, Y.; Sun, K.; Ouyang, J. Solution-Processed Metallic Conducting Polymer Films as Transparent Electrode of Optoelectronic Devices. *Adv. Mater.* **2012**, *24* (18), 2436–2440.

(30) Bubnova, O.; Khan, Z. U.; Wang, H.; Braun, S.; Evans, D. R.; Fabretto, M.; Hojati-Talemi, P.; Dagnelund, D.; Arlin, J.-B.; Geerts, Y. H.; Desbief, S.; Breiby, D. W.; Andreasen, J. W.; Lazzaroni, R.; Chen, W. M.; Zozoulenko, I.; Fahlman, M.; Murphy, P. J.; Berggren, M.; Crispin, X. Semi-Metallic Polymers. *Nat. Mater.* **2013**, *13* (1), 190–194.

(31) Bubnova, O.; Crispin, X. Towards Polymer-Based Organic Thermoelectric Generators. *Energy Environ. Sci.* **2012**, *5* (11), 9345–9362.

(32) Kim, N.; Kang, H.; Lee, J.-H.; Kee, S.; Lee, S. H.; Lee, K. Highly Conductive All-Plastic Electrodes Fabricated Using a Novel Chemically Controlled Transfer-Printing Method. *Adv. Mater.* **2015**, *27* (14), 2317–2323.

(33) Kim, Y. H.; Sachse, C.; MacHala, M. L.; May, C.; Müller-Meskamp, L.; Leo, K. Highly Conductive PEDOT:PSS Electrode with Optimized Solvent and Thermal Post-Treatment for ITO-Free Organic Solar Cells. *Adv. Funct. Mater.* **2011**, *21* (6), 1076–1081.

(34) Badre, C.; Marquant, L.; Alsayed, A. M.; Hough, L. A. Highly Conductive poly(3,4-ethylenedioxythiophene):Poly (styrenesulfonate) Films Using 1-Ethyl-3-Methylimidazolium Tetracyanoborate Ionic Liquid. *Adv. Funct. Mater.* **2012**, *22* (13), 2723–2727.

(35) Wei, Q.; Mukaida, M.; Naitoh, Y.; Ishida, T. Morphological Change and Mobility Enhancement in PEDOT:PSS by Adding Co-Solvents. *Adv. Mater.* **2013**, *25* (20), 2831–2836.

(36) Wei, Q.; Mukaida, M.; Kirihara, K.; Naitoh, Y.; Ishida, T. Recent Progress on PEDOT-Based Thermoelectric Materials. *Materials* **2015**, *8* (2), 732–750.

(37) Massonnet, N.; Carella, A.; Jaudouin, O.; Rannou, P.; Laval, G.; Celle, C.; Simonato, J.-P. Improvement of the Seebeck Coefficient of PEDOT:PSS by Chemical Reduction Combined with a Novel Method for Its Transfer Using Free-Standing Thin Films. *J. Mater. Chem. C* **2014**, *2* (7), 1278–1283.

(38) Patel, S. N.; Chabinyc, M. L. Anisotropies and Thermoelectric Properties of Semiconducting Polymers. *J. Appl. Polym. Sci.* **2016**, *134* (3), 44403.

(39) Gueye, M. N.; Carella, A.; Massonnet, N.; Yvenou, E.; Brenet, S.; Faure-Vincent, J.; Pouget, S.; Rieutord, F.; Okuno, H.; Benayad, A.; Demadrille, R.; Simonato, J.-P. Structure and Dopant Engineering in PEDOT Thin Films: Practical Tools for a Dramatic Conductivity Enhancement. *Chem. Mater.* **2016**, *28* (10), 3462–3468.

(40) Petsagkourakis, I.; Pavlopoulou, E.; Portale, G.; Kuropatwa, B. A.; Dilhaire, S.; Fleury, G.; Hadziioannou, G. Structurally-Driven Enhancement of Thermoelectric Properties within Poly(3,4-Ethylenedioxythiophene) Thin Films. *Sci. Rep.* **2016**, *6*, 30501.

(41) Massonnet, N.; Carella, A.; de Geyer, A.; Faure-Vincent, J.; Simonato, J.-P. Metallic Behaviour of Acid Doped Highly Conductive Polymers. *Chem. Sci.* **2015**, *6* (1), 412–417.

(42) Fabretto, M. V.; Evans, D. R.; Mueller, M.; Zuber, K.; Hojati-Talemi, P.; Short, R. D.; Wallace, G. G.; Murphy, P. J. Polymeric Material with Metal-like Conductivity for next Generation Organic Electronic Devices. *Chem. Mater.* **2012**, *24* (20), 3998–4003.

(43) Park, B. T.; Park, C.; Kim, B.; Shin, H.; Kim, E.; Park, T. Flexible PEDOT Electrodes with Large Thermoelectric Power Factors to Generate Electricity by the Touch of Fingertips. *Energy Environ. Sci.* **2013**, *6* (3), 788–792.

(44) Cho, B.; Park, K. S.; Baek, J.; Oh, H. S.; Koo Lee, Y. E.; Sung, M. M. Single-Crystal Poly(3,4-Ethylenedioxythiophene) Nanowires with Ultrahigh Conductivity. *Nano Lett.* **2014**, *14* (6), 3321–3327.

(45) Zhou, J.; Mulle, M.; Zhang, Y.; Xu, X.; Li, E. High-Ampacity Conductive Polymer Microfibers as Fast Response Wearable Heaters and Electromechanical Actuators. *J. Mater. Chem. C* **2016**, *4* (6), 1238–1249.

(46) Ouyang, J.; Xu, Q.; Chu, C.; Yang, Y.; Li, G.; Shinar, J. On the Mechanism of Conductivity Enhancement in Poly(3,4-Ethylenedioxythiophene):poly(styrene Sulfonate) through Solvent Treatment. *Polymer* **2004**, *45* (25), 8443–8450.

(47) Lin, Y.; Ni, W.; Lee, J. Effect of Incorporation of Ethylene Glycol into PEDOT : PSS on Electron Phonon Coupling and Conductivity. *J. Appl. Phys.* **2015**, *117* (21), 21501.

(48) De, S.; Coleman, J. N. Are There Fundamental Limitations on the Sheet Resistance and Transmittance of Thin Graphene Films ? *ACS Nano* **2010**, *4* (5), 2713–2720.

(49) Sorel, S.; Bellet, D.; Coleman, J. N. Relationship between Material Properties and Transparent Heater Performance for Both Bulk-like and Percolative Nanostructured Networks. *ACS Nano* **2014**, *8* (5), 4805–4814.

(50) Nardes, A. M.; Kemerink, M.; Kok, M. M. De; Vinken, E.; Maturova, K.; Janssen, R. A. J. Conductivity , Work Function , and Environmental Stability of PEDOT : PSS Thin Films Treated with Sorbitol. *Org. Electron.* **2008**, *9* (5), 727–734.

(51) Savage, N. Optical Adhesives. *Nat. Photonics* **2009**, *3* (7), 418–419.

SYNOPSIS

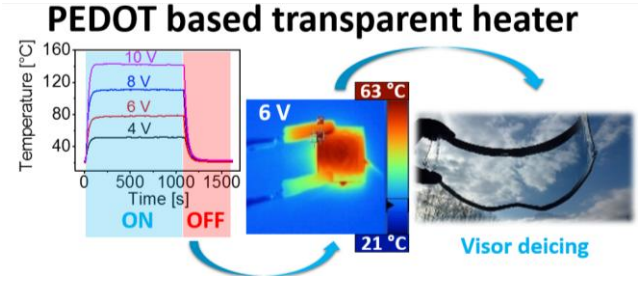
PEDOT based transparent heater
Temperature [°C]
160
120
80
40
10 V
8 V
6 V
4 V
0
500
1000
1500
Time [s]
ON
OFF
6 V
63 °C
21 °C
Visor deicing